Turbulent Channel Flow Simulation Using LES Dynamic Model

Hazm Omran
Libyan Academy

Ali EL SHRIF
Faculty of Engineering, Elmergib University
amelshrif@elmergib.edu.ly

Abstract—**Turbulent flow modelling has increasingly become one of the main scientific research occupations, seeking to develop a universal modelling approach that can describe accurately the dynamics of all turbulent flow scales. Modern attempts try to bring together two main objectives; the applicability of the turbulent flow models to complex flow configurations of industrial interest as well as reducing the computational costs needed for their resolution. Large Eddy Simulation (LES) modelling approach has many promising features among all other turbulent flow modelling approaches such as RANS or DNS. In this study, LES modelling approach has been demonstrated and applied to turbulent channel flow at moderate Reynolds number $Re_\tau = 180$ using Fluent solver. The obtained turbulent flow statistics were compared to their corresponding values of a detailed, well resolved DNS simulation. The obtained LES turbulent flow statistics have an acceptable trend to those of the reference DNS results, which reflects the validity of the LES approach to model turbulent flows accurately and encourages its use in predicting turbulent motion for industrial and engineering applications.**

Index Terms: **turbulence, turbulence modelling, DNS, LES.**

I. INTRODUCTION

Scientific interest in turbulence began when Reynolds (1883) had described the structure of turbulence with its whirls of different sizes and discovered experimentally the effect of the relative strength of inertia to viscous forces in determining the flow regime. Thus leading to the definition of Reynolds number whose value determines when the flow transits from laminar to turbulent state. For decades, research in fluid mechanics remained confined to analytical theory and experiments. Progress in analytical theory rapidly encountered limits due to the complexity, in particular nonlinearity, of the problem, for which an analytical solution can only be obtained for very simple flows. Experimental research has been conducted for many years and is still a method of fundamental importance [1]. Any flow phenomenon in nature whether, laminar or turbulent, is governed by the Navier-Stokes equations which express the conservation of mass, momentum and energy of the flow.

Received 24 Nov, 2018; revised 26 Dec , 2018; accepted 29 Dec, 2018.

Available online December 30, 2018.

The advances achieved in numerical techniques as well as the high performance computing facilities used to solve these equations has made the numerical simulations of turbulent flows an important research tool in studying the basic physics of turbulence. Three approaches can be followed to solve numerically these equations for turbulent flows: Direct numerical simulation (DNS), Reynolds-averaged Navier-Stokes simulation (RANS), and Large-eddy simulation (LES).

The DNS is the direct approach to numerically solve turbulent flow problems and consists in solving the Navier-Stokes equations for all the spatial and temporal scales present in the flow. When it can be applied, DNS is unrivalled in accuracy and in the level of description provided. However, as even the smallest scales where the viscous dissipation takes place have to be resolved, the computational grid needs to be very fine. Even more, as the Reynolds number becomes larger, the amount of scales in a turbulent flow increases and the computational mesh has to be refined dramatically. It can actually be shown that the computational cost of a DNS simulation scales with Re^3 [2]. Thus, to increase the Reynolds number by a factor of two, the computational effort must increase by at least a factor of eight, therefore the feasibility of DNS remains limited to low Reynolds number flows [3]. Furthermore, DNS uses generally high-order accurate numerical schemes for which the extension to complex geometries is not straightforward. DNS may thus be a very powerful tool for fundamental analysis of flows at low Reynolds number and in simple geometries, but is far from being applicable to computations of industrial interest where highly distorted meshes are prevalent and the Reynolds number is typically three orders of magnitude larger.

In order to reduce the amount of scales to be resolved in a turbulent flow, RANS approach considers the application of an ensemble mean operator to the Navier-Stokes equations to separate the mean flow field from the fluctuating turbulent flow field. In practice the ensemble averaging is carried out by time averaging in case of inhomogeneous turbulence and by space averaging in case of homogeneous turbulence so that the flow is only resolved in terms of time-averaged and space-averaged variables [4]. The averaging of the nonlinear terms introduces new unknowns for which closure needs to be obtained via an appropriate turbulence model. A large variety of turbulence models has been derived over the years, starting with simple algebraic models and ending

with more sophisticated two-equation models [5],[6],[7]. The main drawback of the RANS approach is that the quality of the results depends to a large extent on the appropriateness of a turbulence model to cope with a particular flow configuration, stressing thus the importance of experience and practice in the choice of the best model [2]. For statistically stationary turbulence, RANS nevertheless provides an unbeatable ratio between flow prediction quality and computational cost, which made it to become the favourite computational method for many industrial simulations.

Unsteady phenomena, however, introduces a fundamental uncertainty into the RANS framework. Reynolds-averaging presupposes that the flow is statistically stationary. At the very least, the time-scale associated with the organized unsteady structures must be substantially larger than the time-scale of the turbulent fluctuations. This condition may be satisfied for low-frequency motion such as dynamic stall, but not necessarily in flows exhibiting unsteady separation and reattachment, transition or vortex interaction, where RANS methods reach their limit [8]. Therefore, alternative methods to circumvent the stationary assumption of RANS needed to be found.

The last approach, LES, lies between DNS and RANS in terms of computational cost and resolved scales, and motivated by the limitations of each of these approaches. In LES, the large scales of turbulent motion are resolved, while the effect of the small scales is modelled. The separation between large and small scales is obtained by application of a spatial filter to the Navier-Stokes equations yielding the filtered Navier-Stokes equations with corresponding filtered variables. The filter width, which is a characteristic length-scale, determines the scales that are still present in the filtered variables (resolved scales, larger than the filter width) and the ones that are removed (sub grid scales, smaller than the filter width). The filtering of the nonlinear terms introduces new unknown quantities, well known as sub-grid scale (SGS) terms, which have to be modelled to close the system of equations [9].

LES approach represents large scale unsteady motion explicitly, so it can be expected to be more accurate and reliable than the RANS approach for flows with significant large-scale unsteadiness. An essential challenge in LES is the modelling of the sub-grid scale (SGS) stresses, representing the interactions between the large (above the filter width) and small (below the filter width) scales in the filtered Navier-Stokes equations. A remarkable research effort has led to a wide variety of SGS models [8],[10], [11],[12], [13]. Arguably the most popular class of LES models is the eddy-viscosity type, based on (variants of) the Smagorinsky model. These models have several limitations, however, including poor correlation coefficients in a priori tests, inability to provide backscatter; excessive damping of resolved structures and bad SGS stresses prediction near the wall region [4], [14]. Some of these limitations are circumvented by using a dynamic procedure in calculating the Smagorinsky constant, yielding the dynamic sub-grid scale eddy-viscosity model introduced by Germano and others [14], and used in many studies [11],[15],[16]. In the present study, the dynamic model formulation has been outlined and applied to a plan turbulent channel flow. The objective of the study resides on demonstrating the power of the LES approach in generating the correct turbulent flow dynamics such as that captured by the detailed turbulent flow simulation using the DNS approach.

II. LES THEORY

For a Newtonian incompressible flow, the governing equations of fluid motion (Navier-Stokes equations) can be written in a Galilean reference frame as:

$$\frac{\partial u_i}{\partial x_i} = 0. \tag{1}$$

$$\frac{\partial u_i}{\partial t} + \frac{\partial (u_i u_j)}{\partial x_j} + \frac{\partial p}{\partial x_i} + \frac{\partial \tau_{ij}}{\partial x_j} - \frac{1}{Re_\tau} \frac{\partial^2 u_i}{\partial x_j^2} = 0. \tag{2}$$

Which when solved completely using the DNS approach, gives a detailed description of all turbulent flow scales in the flow. Large-eddy simulation (LES) is a technique intermediate between DNS and RANS, which relies on computing accurately the dynamics of the large eddies while modelling the small, sub-grid scales of motion. This method is based on the consideration that, while the large eddies are flow-dependent, the small scales tend to be more universal, as well as isotropic. Furthermore, they react more rapidly to perturbations, and recover equilibrium quickly. Thus, the modelling of the sub-grid scales is significantly simpler than that of the large scales, and can be more accurate.

To separate the large from the small scales, LES is based on the definition of a filtering operation: a filtered (resolved or large-scale) variable, denoted by an over-bar, is defined by:

$$\bar{\emptyset}(x,t) = G * \emptyset = \int_{-\infty}^{+\infty} \emptyset(x',t)\, G(x-x')\, dx'. \tag{3}$$

Where G is the filter function characterized by the filter width Δ which determines the size of the largest eddy removed by the filtering operation. The filter function G is a function of $(x-x')$ only, and hence, differentiation and filtering operation commute [7]. There are many filter functions that can be used in this context, among which is the spectral cut-off filter; the Gaussian filter and the top hate filter. The most commonly-used filter functions are the sharp Fourier cut-off filter, defined by:

$$G(x-x') = \frac{\sin\left(\pi \frac{(x-x')}{\bar{\Delta}}\right)}{\left(\pi \frac{(x-x')}{\bar{\Delta}}\right)}. \tag{4}$$

In LES the filtering operation Eq. (3) is applied formally to the governing equations Eq. (1) and Eq. (2); this results in the filtered equations of motion, which are solved in the LES. Applying the filtering operation to the governing equations leads to the filtered Navier-Stokes equations:

$$\frac{\partial \bar{u}_i}{\partial x_i} = 0. \tag{5}$$

$$\frac{\partial \bar{u}_i}{\partial t} + \frac{\partial (\bar{u}_i \bar{u}_j)}{\partial x_j} + \frac{\partial \bar{p}}{\partial x_i} + \frac{\partial \tau_{ij}}{\partial x_j} - \frac{1}{Re} \frac{\partial^2 \bar{u}_i}{\partial x_j^2} = 0. \tag{6}$$

The filtered Navier-Stokes equations written above govern the evolution of the large, energy-carrying, scales of motion. The effect of the small scales appears through a sub-grid scale (SGS) stress term τ_{ij}, which must be modelled to achieve closure of the system of equations.

Where $$\tau_{ij} = \overline{u_i u_j} - \bar{u}_i \bar{u}_j$$

The main role of the sub-grid scale model is, therefore, to remove energy from the resolved scales, mimicking the drain that is associated with the energy cascade. Most sub-grid scale models are eddy-viscosity models of the form that relate the sub-grid-scale stresses τ_{ij} to the resolved strain-rate tensor [17]:

$$\tau_{ij} - \tfrac{1}{3} \delta_{ij} \tau_{kk} = -2 \nu_\tau \bar{S}_{ij}. \tag{7}$$

Where

$$\bar{S}_{ij} = \frac{1}{2}\left(\frac{\partial \bar{u}_i}{\partial x_j} + \frac{\partial \bar{u}_j}{\partial x_i}\right)$$

In most cases the equilibrium assumption (namely, that the small scales are in equilibrium, and dissipate entirely and instantaneously all the energy they receive from the resolved ones) is made to simplify the problem further and obtain an algebraic model for the eddy viscosity [8]:

$$\nu_\tau = C_s \bar{\Delta}^2 |\bar{S}|. \tag{8}$$

This model is known as the "Smagorinsky model". Where $|\bar{S}| = (2\bar{S}_{ij}\bar{S}_{ij})^{1/2}$, and C_s is the Smagorinsky constant, which takes the value 0.18 for the case of homogenous isotropic turbulent flows. In the presence of shear, near solid boundaries or in transitional follows, however, it has been found that C_s must be decreased. This has been accomplished by various types of *ad hoc* corrections such as van Driest damping or intermittency functions [16]. Although this damping function produces the desired results for some turbulent flow configurations, it is difficult to justify in the context of LES and is difficult to extend to complex flows [14]. These requirements led to the dynamic model approach, in which an appropriate local value of the Smagorinsky coefficient has to be computed dynamically from the resolved field as the calculation progresses rather than prescribed *a priori.*

The concept of the dynamic model was originally proposed by Germano *and others* [14] and it has been successfully used to study a variety of complex inhomogeneous flows. In this approach, the small eddies are filtered by the grid filter, then the relatively small eddies in the LES resolved field are again filtered by a test filter. These two filters are assumed to be similar. In order to make the Smagorinsky model work for both scales, the cut-off of both filters has to be located in the inertial range of the turbulent energy spectrum. A test filtering operation is given by:

$$\tilde{\emptyset}(x,t) = \hat{G} * \emptyset = \int_{-\infty}^{+\infty} \emptyset(x,t)\, \hat{G}(x - x')\, dx'. \tag{9}$$

In which the test filter width $\hat{\bar{\Delta}}$ be larger than the width of the original grid filter $\bar{\Delta}$. After applying the test filter to the grid filtered equations, the sub-grid scale stress that must be modelled at the test-filter level LES is given by:

$$T_{ij} = \widehat{\bar{u}_i \bar{u}_j} - \hat{\bar{u}}_i \hat{\bar{u}}_j. \tag{10}$$

Then Germano identity which expresses the Leonard stress in terms of both the sub-grid scale Reynolds stress τ_{ij} and the test filtered sub-grid scale stress T_{ij} is obtained:

$$L_{ij} = T_{ij} - \hat{\tau}_{ij}. \tag{11}$$

Where $$L_{ij} = \widehat{\bar{u}_i \bar{u}_j} - \hat{\bar{u}}_i \hat{\bar{u}}_j - \widehat{\bar{u}_i \bar{u}_j} + \widehat{\bar{u}_i \bar{u}_j}$$

$$L_{ij} = \widehat{\bar{u}_i \bar{u}_j} - \hat{\bar{u}}_i \hat{\bar{u}}_j$$

This stress represents the contribution to the Reynolds stresses of turbulent scales whose length is intermediate between the grid filter width and the test filter width. The basic assumption that leads to the dynamic model is that the Smagorinsky eddy viscosity model applies on both filter levels with the same value of parameter C_s.

$$\tau_{ij} - \tfrac{1}{3} \delta_{ij} \tau_{kk} = -2 C_s \bar{\Delta}^2 |\bar{S}| \bar{S}_{ij}. \tag{12}$$

$$T_{ij} - \tfrac{1}{3} \delta_{ij} T_{kk} = -2 C_s \hat{\bar{\Delta}}^2 \left|\hat{\bar{S}}\right| \hat{\bar{S}}_{ij}. \tag{13}$$

Then

$$L_{ij} - \tfrac{1}{3} \delta_{ij} L_{kk} = -2 C_s \hat{\bar{\Delta}}^2 \left|\hat{\bar{S}}\right| \hat{\bar{S}}_{ij} + 2 C_s \bar{\Delta}^2 \widehat{|\bar{S}| \bar{S}_{ij}}. \tag{14}$$

Which, when contracted with $\bar{S}_{ij}$ leads to an expression for the eddy viscosity constant in terms only of the resolved velocity field:

$$C_s = \frac{L_{ij} \bar{S}_{ij}}{M_{kl} \bar{S}_{kl}}. \tag{15}$$

Where the tensor M_{ij} is given by:

$$M_{ij} = -2C_s\hat{\bar{\Delta}}^2\left|\hat{\bar{S}}\right|\hat{\bar{S}}_{ij} + 2C_s\bar{\Delta}^2\widehat{|\bar{S}|\bar{S}_{ij}}. \qquad (16)$$

Lilly [77] suggested an improvement to compute the optimum for C_s in the least-squares sense, which is equivalent to taking the scalar product of Eq. (14) with M_{ij} yielding:

$$C_s = \frac{L_{ij}M_{ij}}{M_{kl}\bar{S}_{kl}}. \qquad (17)$$

However, it was found that C_s may change sign and takes negative values or may become indeterminate if the denominator is zero. To overcome the problems created by the large negative eddy viscosities and zero denominators, one can implement an average over homogeneous directions [16], [18]:

$$C_s = \frac{\langle L_{ij}M_{ij}\rangle}{\langle M_{kl}M_{kl}\rangle}. \qquad (18)$$

III. NUMERICAL EXPERMIMENT

Turbulent channel flow has been extensively used as scientific research tool to validate and test the veracity of turbulent flow simulations either using the DNS approach or other turbulence modelling [3], [19], [20]. In order to verify the capacity of the LES approach in generating turbulent flow motion correctly, a turbulent channel flow at moderate Reynolds number $Re_\tau = 180$ has been considered. The Fully developed turbulent channel flow is homogenous in the streamwise and spanwise directions, and periodic boundary conditions are used in these directions. The no slip boundary condition has been imposed on the upper and lower channel walls. The channel geometry has been chosen as to include the largest eddies in the flow which is guaranteed as turbulent fluctuations become uncorrelated at about one half period in the homogenous directions. A staggered grid is used in the normal direction to insure high grid resolution needed to capture fine turbulent flow scales present near the wall region. In Fluent solver the grid filter width is computed according to the volume of the computational cell $\bar{\Delta} = V^{1/3}$. The test filter width used by Fluent solver is equal to twice the grid width $\bar{\Delta}$. The channel geometry and computational resolution used are given by Table (1).

Table 1. Geometry and Resolution

L_x^+	L_y^+	L_z^+	Δx^+	Δy_{min}^+	Δy_{max}^+	Δz^+
1134	360	576	12.46	0.882	11.43	12.26

The turbulent flow simulations have been carried out using Fluent solver with computational options listed in the Table (2).

Table 2. Computational Options

Re_τ	Δt (s)	$\mu\ (N\cdot s/m^2)$	$\rho\ (Kg/m^3)$
180	0.001	0.000555	1.0
P-V Coupling			Simplic
Turbulent Model			LES Dynamic Model
Time Integration			2^{nd} order Implicit

To generate turbulent flow motion, an initial condition of velocity field obtained from a fully developed steady turbulent channel flow simulation is used as an inlet condition. The built-in function "Spectral Synthesiser" has been used to perturb the inlet condition and induce turbulent motion as integrating time succeeds. After the flow has reached the fully developed turbulent state, which can be distinguished by almost constant value of the drag coefficient on channel walls displayed on the monitoring screen, the collection of turbulent velocity field samples starts. Flow statistics are computed using samples of different flow quantities collected over a long integrating time period $(T^+ = 360)$. All flow variables have been non-dimensionalized using the characteristic wall flow variables defined as follows:

$$u_\tau = \sqrt{\frac{\tau_w}{\rho}}\ ; \qquad \delta_v = \frac{\nu}{u_\tau} \qquad ; \qquad t_v = \frac{\nu}{u_\tau^2}$$

Collected flow quantities have been converted in wall units as to become comparable to their corresponding quantities of the reference DNS data. Non-dimensional flow variables have been computed as follows:

$$u^+ = \frac{u}{u_\tau}\ ; \qquad x^+ = \frac{x}{\delta_v}\ ; \qquad t^+ = \frac{t}{t_v}$$

IV. RESULTS AND DISCUSION

Mean turbulent flow statistics have been compared to their corresponding values of the detailed DNS simulation realised by MKM99 (Moser, Kim and Mansour 1999), statistics up to fourth order are presented. Each kind of these statistics gives some details about turbulent flow dynamics and the interactions that occur between turbulent flow structures present in the flow. The results can also give an indication about the resolution accuracy of the different turbulent flow scales generated by the LES model. As the flow reaches fully developed state, the average velocity field becomes independent of homogenous directions and vary only in the normal direction. Large samples of velocity fields have been collected ($N_t = 100$ samples for each flow quantity).

Statistical mean values have been computed using the averaging operator defined by:

$$\bar{\emptyset}(y) = \frac{1}{N_x N_z N_t} \sum_{1}^{N_t} \sum_{1}^{N_x} \sum_{1}^{N_z} \emptyset(x, y, z, t) \qquad (19)$$

Where $N_x = 91$, $N_z = 47$ is the number of grid points in the streamwise and spanwise directions respectively. The computed turbulent flow statistics will be presented together with their corresponding values of the reference DNS data available online [21].

A. *Mean turbulent flow velocity profile*

Figure 1. shows the axial mean velocity profile in wall units traced with the normal distance from the wall through the lower half of the channel. To validate LES results, the corresponding profile of the reference DNS has been traced on the same figure. The two mean axial flow velocity profiles are in good agreement in the near wall region and they diverge slightly from each other as far as $y^+ = 25$. The near wall region is characterized by a strong velocity gradient which results in a high viscous shear rates in this region. In the mid channel region; contrary to the purely parabolic profile of the laminar state; the mean axial turbulent flow has approximately a flat shape. More insight to flow structures can be obtained by tracing the velocity profile in a logarithmic scale as shown by Figure 2. Three dynamic layers can be distinguished, the viscous sub-layer $y^+ \leq 5$, the overlap layer $5 \leq y^+ \leq 30$ and the logarithmic layer $y^+ > 30$. The viscous sub-layer dominates the region too close to the wall where the velocity profile takes a linear character $(u^+ = y^+)$. Throughout this region viscous dissipation and viscous diffusion mechanisms are in equilibrium and dominate turbulent flow activities. The overlap layer behaves as transition region between molecular viscosity dominating region and turbulence dominating region. No theoretically based expression has been given for the mean axial velocity distribution in this layer. The LES mean velocity profile in these two inner layers has an acceptable trend towards the reference DNS mean velocity profile.

Far from the wall $y^+ > 30$, the mean velocity profile has to follow the log law profile due to von Kármán given by:

$$u^+ = \frac{1}{k} \ln y^+ + B \qquad (20)$$

Where $(k = 0.41 , B = 5.2)$ for the considered confined turbulent flow.

The LES mean velocity profile marks some discrepancy towards the log law which probably reflects an inadequate mesh size used in this region.

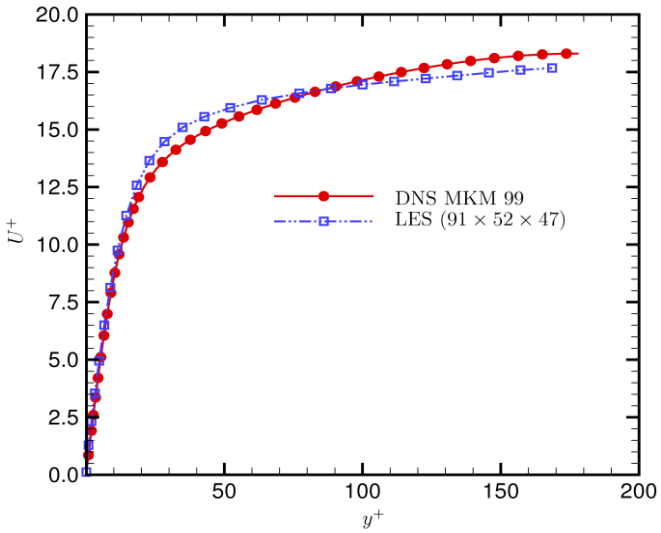

Figure 1. Mean Axial Velocity Profile in Wall Units vs Normal Distance from the Wall

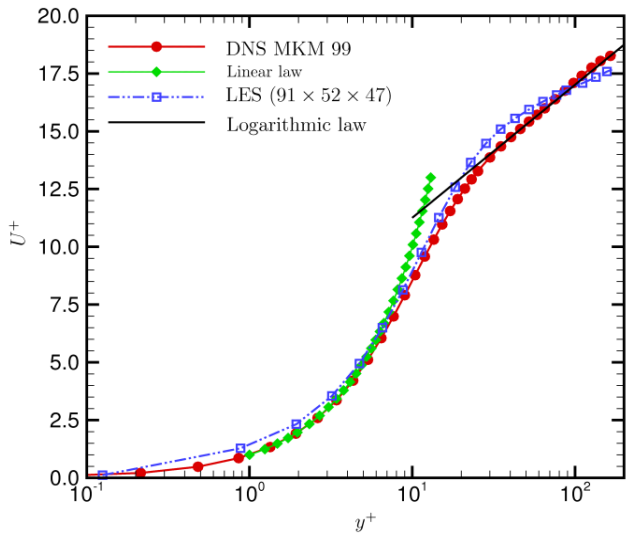

Figure 2. Mean Axial Velocity Profile vs Normal Distance from the Wall in Logarithmic Scale.

B. *Turbulent intensities*

Turbulence intensities are given by the root mean square of the three components of velocity fluctuations or simply the square root of the diagonal elements of the Reynolds stress tensor.

Figure 3. shows turbulence intensities generated by the LES model normalized by the wall-shear velocity and compared to their corresponding profiles of the reference DNS. In the near wall region $(y^+ < 17)$, the axial **urms** component given by the LES model matches well the **urms** profile given by the reference DNS with some discrepancy occurs after reaching a pick value at $(y^+ \approx 15)$. The other two components **vrms** and **wrms** deviate slightly from their corresponding reference values throughout the region $(18 < y^+ < 70)$, while an unexpected behavior occur to the three components of

turbulent intensities in the mid region between channel walls, where their values increasing instead of decreasing.

The pick value of the three components marks the most active turbulent flow region where turbulent production mechanisms take place at about $(y^+ \approx 15)$. This region is the theatre of the maximum containing energy events in the flow. As reported in [19], this region will be shifted slightly towards the wall as Reynolds number increases.

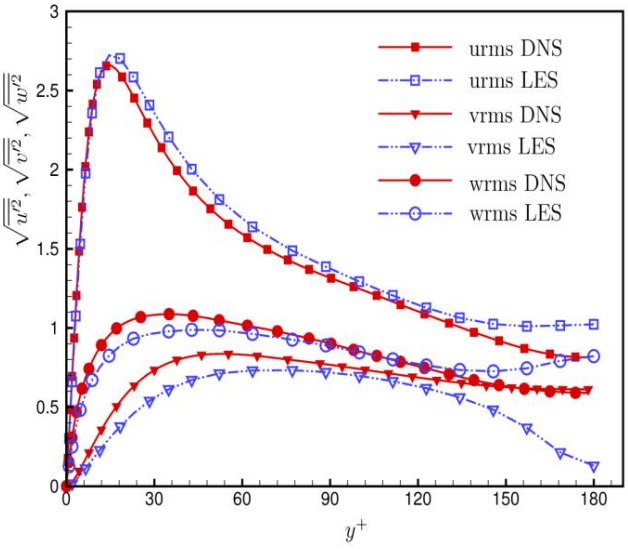

Figure 3. Turbulent Intensities

C. *Turbulent and viscous shear stresses*

The total shear stress varies linearly across the channel and is everywhere equal to the sum of the mean viscous and Reynolds stress contributions [20]. Thus, theoretical profile of the total shear stress en terms of its viscous and turbulent stress contributions is given by:

$$\tau_t^+ = \tau_v^+ + \tau_r^+$$
$$\tau_t^+ = \frac{d\bar{u}^+}{dy^+} - \overline{u'^+ v'^+} \qquad (21)$$

This provides that the viscous and Reynolds stress don't individually vary linearly. Figure 4. shows the total shear stress generated by the LES compared to the theoretical profile given by Eq. (21). The perfect fitness of the LES generated total stress profile with the theoretical one insures that the collected LES statistics belongs to a fully developed turbulent flow and reflects also the adequacy of the samples size used to calculate turbulent flow statistics.

Figure 5. demonstrates the mutual effect played by each shear stress contribution to the total stress distribution across the channel. The importance of the mean viscous stress is confined to a thin region near the boundary. Thus only layers of fluid very close to the wall feel the retardation effect of the solid boundary at the molecular level. Away from the wall the Reynolds stress contribution is dominant and therefore the molecular momentum flux is replaced by a turbulent momentum flux.

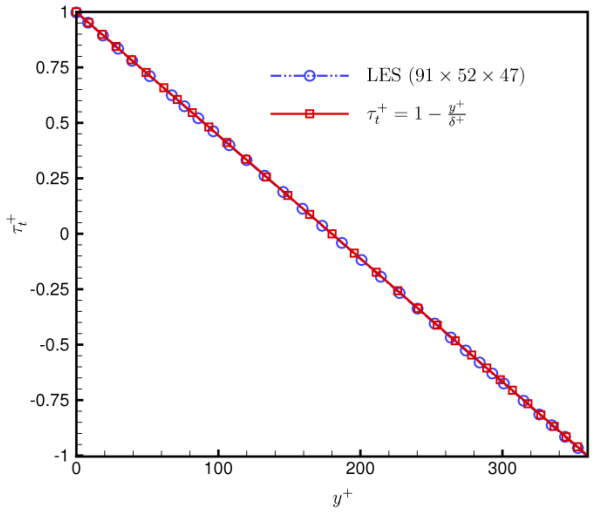

Figure 4. Total Shear Stress Distribution in Wall Units.

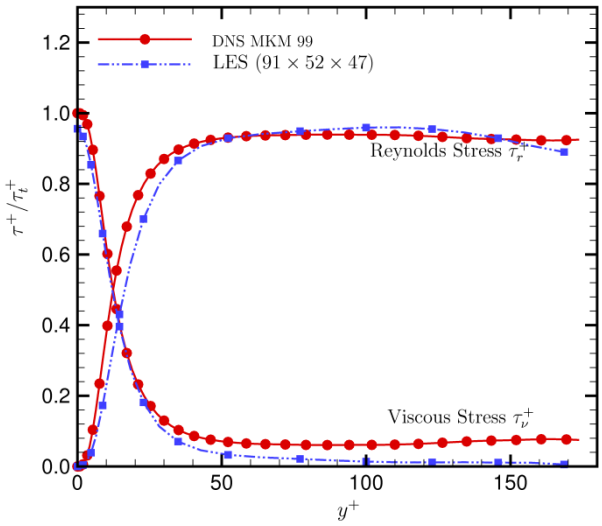

Figure 5. Viscous and Turbulent Shear Stresses Distribution.

Reynolds stress presents an anti-symmetric profile across the channel with $\overline{u'^+ v'^+} > 0$ on the upper half and $\overline{u'^+ v'^+} < 0$ on the lower half which indicates that the turbulent momentum flux is always towards the wall in each half of the channel. The peak value of $u'^+ v'^+$ occurs at $(y^+ \approx 15)$. Reynolds stress varies almost exactly linearly through the central region where viscous stress contribution is negligible. The situation in Figure 5. is reflected in the balance of forces in turbulent channel flow, viscous forces are significant only in the near wall region while forces originating in turbulent momentum transport dominate the reminder of the channel.

D. *High order statistics*

High order moments such as skewness and flatness of fluctuating velocity field reveal the underlying turbulence mechanisms that maintain and generate turbulent motion. The skewness coefficient of the fluctuating velocity field is defined by:

$$S_{u_i} = \frac{\overline{u_i'^3}}{(\overline{u_i'^2})^{3/2}}. \qquad (22)$$

For a turbulent velocity field, this coefficient measures the deviation of fluctuating velocity components from the Gaussian distribution and gives an indication about their direction of motion. Figure 6. shows skewness coefficients of the fluctuating velocity components across the channel compared to the corresponding skewness coefficients reported in the reference DNS. The overall behaviour of the skewness coefficients provided by the LES model is in good agreement with the reference values. In the near wall region $(y^+ \approx 14.5)$, the coefficient S_u is positive, which corresponds to a high probability that $u' > 0$. After that position, S_u becomes negative which corresponds to $u' < 0$ almost everywhere. According to the profile of skewness of v', there exist strong positive v' motion for $(y^+ \leq 10)$, weak negative v' motion for $(10 < y^+ \leq 20)$, and then strong v' motion for $(y^+ \geq 20)$. The most energetic Reynolds stress producing events take place when strong negative v' motion coincides with a strong positive u' motion or vice versa. The skewness coefficient of w' component does not agree with that of the reference DNS and does not has a Gaussian distribution which should be zero because of the reflection symmetry of the solution of the Navier-Stokes equations.

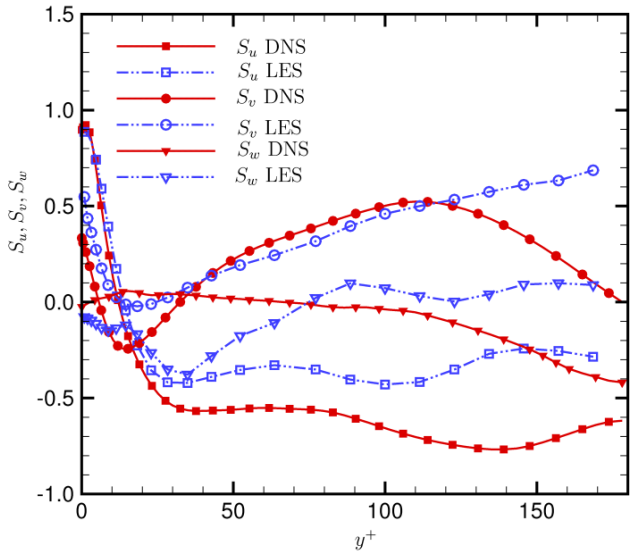

Figure 6. Skewness Coefficients of the Fluctuating Velocity Field.

The flatness coefficient of a turbulent velocity field measures the probability distribution of velocity fluctuations about their mean value and is given by:

$$F_{u_i} = \frac{\overline{u_i'^4}}{(\overline{u_i'^2})^2} \qquad (23)$$

The higher value of F_{u_i} indicates an intermittent character of u_i'. Flatness coefficients of the fluctuating velocity field produced by the LES model are shown by Figure 7. together with their corresponding DNS results. The flatness coefficients of the three fluctuating velocity components present a highly intermittent character in the near wall region while they tend to behave as a Gaussian profile as far as ($y^+ \geq 30$).

However, the computed skewness and flatness factors of the fluctuating velocity field indicate that the adequacy of the sample size used to calculate these higher order statistics is only marginal, as indicated by the oscillations in their profiles.

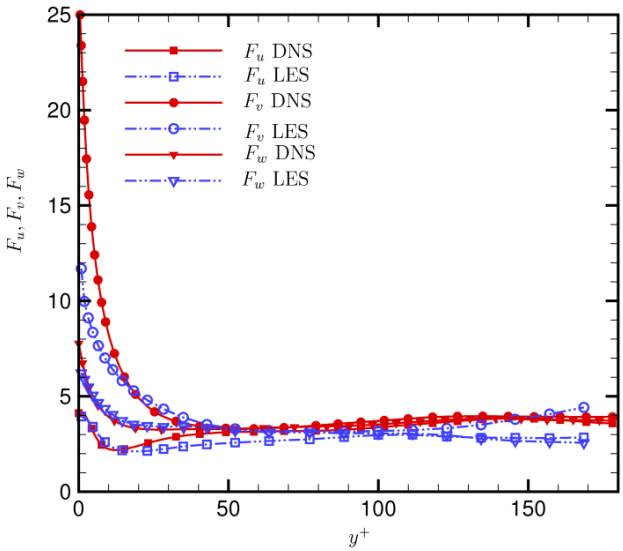

Figure 7. Flatness Coefficients of the Fluctuating Velocity Field.

CONCLUSION

In the current study, the dynamic LES turbulence modelling approach has been applied to solve turbulent channel flow problem and successfully generated turbulent motion with a precision close to that given by a detailed DNS simulation. The obtained turbulent channel flow statistics are in good agreement with those given by the reference DNS. Therefore LES model can be considered as a low order alternative of the full Navier-Stokes equations, where the number of degree of liberty associated to the considered turbulent flow problem has been considerably reduced.

The LES turbulence modelling approach impeded in Fluent solver is a promising tool towards turbulent flow simulation with low computational costs. Essential features of turbulent bounded flow including turbulent boundary layer, turbulent stress production and the sweep and ejection events associated to the turbulence production cycle have been correctly produced by the LES model. The position in wall units where the maximum turbulent energy occurs is close to the value reported in [19]. This location marks the zone of the

strong turbulent activities where turbulence production cycle takes place.

Except some discrepancies of the **rms** values of turbulent velocity fluctuations in the mid zone between channel walls which can be attributed to an inadequate resolution used in this region, the overall results are more than satisfactory. Therefore, the study encourages the use of the LES modelling approach embedded in the Fluent solver as an accurate tool for the simulation of practical turbulent flow problems.

REFERENCES

[1] P. S. Bernard, J. M. Wallace , "*Turbulent Flow, Analysis, Measurment, and prediction*'', John Willy&Sons, 2002.

[2] S. B. Pope "*Turbulent Flows, University press''*, Cambridge, 2009.

[3] J. Kim, P. Moin and R. Moser, "*Turbulence statistics in fully developed channel flow at low Reynolds number'',* J. Fluid Mech., pp. 133-166, 1987.

[4] Wilcox, "*Turbulence Modeling for CFD'',* La Canada, CA:DCW Industries, 1993.

[5] C. G. Speziale, T. B. Gatski, T. B., "*On explicit algebric stress models for complex turbulent flows*'', J. of Fluid Mechanics , pp. 254, 59-78, 1993.

[6] B. E. Launder, G. J. Reece, and W. Rodi, *"Progress in the development of a Reynolds stress turbulence closure''*, J. Fluid Mechanics , pp. 68, 537-566, 1975.

[7] C. G. Speziale, R. Abide and E. Anderson "*Critical evaluation of two - equation models for near wall turbulence.,*'' AIAA Journal, pp. 30, 324-331, 1992.

[8] R. v. Kaenel, "*Large-eddy simulations of compressible flows using the finit volume method,*'' Switzerland: Swiss Federal Institute of Technology Lausanne, 2003.

[9] P. Sagaut, *« Large-Eddy Simulation for incompressible Flows - An Introduction, »* Springer-Verlag, 2005.

[10] K. Akselvoll , and P. Moin, " *Large eddy simulation of turbulent confined coannular jets*,'' J. Fluid Mech., pp. 387-411, 1996.

[11] E. Montreuil, "*Simulation numérique pour l'aérothérmique avec des modéles de sous-maille*,'',Phd Thesis, Paris, 2000.

[12] J. Meyers, " *Accuracy of Large-Eddy Simulation Stratgies*,'' Heverlee (Belgie): Katholieke Universiteit Leuven - Faculteit ToegepasteWetenschappen, 2004.

[13] P. Comte, "*Analysis of Turbulent Flows in Large Eddy Simulations*,'' Roscoff, France, 2007.

[14] M. Germano, U. Piomelli , P. Moin and W. H. Cabot, "*A dynamic subgrid-scal eddy viscosity model,''* Phys. Fluids , pp. 1760-1764, 1991.

[15] S. S. Collis , Y. Chang, "On the use of LES with dynamic subgrid-scall model for optimal control of wall bounded turbulence.,'' chez International Conference on DNS/LES, New Brunswick, NJ/USA, 1999.

[16] Y. Chang, "*Approximate models for optimal control of turbulent channel flow,*'' Phd thesis, Rice University, 2000.

[17] U. Piomelli,A. Scotti, and E. Balaras, "*Large-Eddy Simulations of Turbulent Flows,from Desktop to Supercomputer*,'' Springer-Verlag, Berlin Heidelberg, 2001.

[18] U. Piomelli, "*High Reynolds number calculations using the dynamic subgrid-scale stress model*,'' Phys. of fluids, vol. A 5, pp. 1484-1490, 1993.

[19] M. Fischer , J. Jovanovic, and F. Durst, "*Reynolds number effects in the near-wall region of turbulent channel flow*,'' Phys. Fluids, vol. 13, n° 16, pp. 1755-1767, 2001.

[20] R. Moser, J. Kim, and N. Mansour, "*Direct numerical simulation of turbulent channel flow up to Re=590*,'' Phys. Fluids, vol. 11, n° 14, pp. 943-945, 1999.

[21] R. Moser, J. Kim, and N. Mansour, "*DNS Data for Turbulent ChannelFlow*,''[Enligne].Available: http://turbulence.ices.utexas.edu/MKM_1999.html.

[22] L. Cordier, A. EL SHRIF , "*Optimal Control of Turbulent Channel Flow using an LES Reduced-Order Model*,'' Révue de Mécanique Appliquée et Théorique , vol. 2, n° 15, pp. 487-500, 2011.

[23] T. Brandt, "*A priori tests on numerical errors in large eddy simulation using fnite differences and explicit fitering*,'' International journal for numerical methods in fluids, 2005.